A Study on Diesel Spray Characteristics for Small-Quantity Injection

Bao, Zhichao; Horibe, Naoto; Ishiyama, Takuji

2018-01-0283

A Study on Diesel Spray Characteristics for Small-quantity Injection

Author, co-author (Do NOT enter this information. It will be pulled from participant tab in MyTechZone)

Affiliation (Do NOT enter this information. It will be pulled from participant tab in MyTechZone)

Abstract

Multi-stage injection with pilot injection and post injection has been widely used for the noise and emissions reduction of diesel engines. Considering many parameters to be decided for optimal combustion, computer simulations such as three dimensional computational fluid dynamics (3D-CFD) and lower dimensional codes should play a role for optimal selection of intervals and quantity ratios. However, the data for the sprays are insufficient for reproducing the actual fuel-air mixture formation process related to pilot and post injection. Hence, there is a need for experimental data with a small-quantity injection. The small-quantity injection is characterized with an injection rate shape similar to a triangle rather than a rectangle. This study is mainly focused on the spray characteristics of diesel sprays in which the entire process is dominated by unsteady injection processes. The effects of injection parameters and nozzle hole diameter on spray penetration, spray angle, and fuel concentration are studied with the help of a rapid compression and expansion machine. A hybrid of shadowgraph and Mie scattering imaging set-up is used to visualize both spray liquid phase and vapor phase at the same time. A high-speed camera with a frame rate of 90,000 fps is used to acquire spray images. Two injectors with a nozzle hole diameter of 0.12 mm and 0.14 mm are used. The studies are performed at the injection pressure of 40, 80, and 120 MPa while environmental temperature of 850 K. The experimental results show that the development of the spray tip is proportional to t and then to $t^{1/2}$ at the later stage, and after the end of the injection, the spray tip penetration is found to follow $t^{1/4}$. Also, the spray liquid penetration, spray dispersion, and air-fuel mixing processes are evaluated and compared with various injection parameters. In addition, the instantaneous behavior of the near-nozzle spray angle is studied carefully in order to provide reliable input data for spray models.

Introduction

Multi-stage injection has been extensively adopted to diesel engines for its advantages on emission and noise reduction. One of the examples is a small amount of injection prior to main injection called pilot injection. Pilot injection shortens the ignition delay of the main injection by producing a high temperature air-fuel mixture which suppresses the combustion noise [1]. Another example is a post injection injected after the main injection. The post injection can help with the oxidization of soot produced during main combustion. Also, the soot reduction can be attributed to splitting the soot producing process by dividing the fuel injected into chambers [2, 3]. While the technology of multi-stage injection strategy progresses, the immense parameters of the multiple injection such as injection timing, pressure, and mass require enormous work for engine performance optimization. Therefore, it is preferred to predict the spray development and combustion process by phenomenological combustion model and 3D-CFD model simulation.

Hiroyasu and Arai proposed the most widely referred empirical equations describing the tip penetration of diesel spray and its break-up timing [4]. According to these equations, the spray tip penetration is a function of t and $t^{1/2}$ before and after break-up timing, respectively. After that, Naber and Sieber studied the effects of gas density and vaporization on spray tip penetration and dispersion [5]. These studies are based on the experimental data acquired by rather long injection where the duration of injection rate increase and decrease can be neglected. Thus, the spray characteristics during the beginning or ending of injection are not of concern. On the other hand, some research noticed the significance of SOI (start of injection) and EOI (end of injection) effects on spray characteristics. J. Kostas et al. supposed that instead of exhibiting a linear dependence on time, spray tip penetration is proportional to $t^{3/2}$ during the initial stage of injection [6]. Although, the theoretical explanation was not available, this study identified that the spray tip experiences a short acceleration during the needle lift timing. However, the EOI effect was not discussed in this research since it dealt with quasi-steady injection. Some research investigated the effect of EOI on spray characteristics. For example, a simple one-dimensional model was proposed and EOI effect on fuel-air mixing was discussed by Musculus et al. [7]. However, this study utilized a square-wave injection pulse to the simulation. In addition, Pickett et al. focused on the ramp-up and -down effect of injection rate to the characteristics of fuel spray. But instead of investigating the effect of unsteady injection rate on spray characteristics, the research was conducted under a nearly top-hat shape injection rate. Also, they indicated that since the injection rate uncertainties were so significant during the initial stage of injection, an educated injection rate based on experience was proposed [8]. In summary, currently, the data required to improve the accuracy of the model is insufficient since most of the studies concerned with diesel spray are concentrated on quasi-steady injection. Hence, this study aimed to investigate the characteristics of small-quantity injection, which do not possess a steady injection duration.

As stated above, the motivation of this study was the lack of data on the characteristics of small-quantity injections. Thus, in this study, the spray tip penetration as well as the spray liquid phase development were observed and investigated under small-quantity injection conditions. In addition, the near-nozzle spray angle, which may be utilized for spray model construction, was compared. Also, in order to evaluate the spray entrainment amount, the spray cone angle

was suggested and calculated. The high pressure and temperature condition in a combustion chamber was created by a rapid compression and expansion machine (RCEM), and diesel fuel was injected into the chamber by a single-hole piezo injector. For the diagnosis of vapor and liquid phases simultaneously, the Mie scattering method was used to identify liquid phase development while shadowgraph imaging method was used to track the vapor phase. Injection pressure and injection mass were varied from 40 MPa to 120 MPa and 0.25 mg to 0.80 mg, respectively. Two single-hole injectors with nozzle diameters of 0.12 mm and 0.14 mm were used to investigate the effect of nozzle diameter to spray characteristics.

Experimental Setup

The main experiment set consisted of the RCEM, an intake charge reservoir, a fuel injection system, a control unit, and a data recording unit. The schematic drawing is shown in Figure 1. A four-stroke single-cylinder diesel engine (Yanmar NFD170, Bore 102 mm, Stroke 105 mm) was the base of the RCEM and the cylinder head was redesigned for optical experiments.

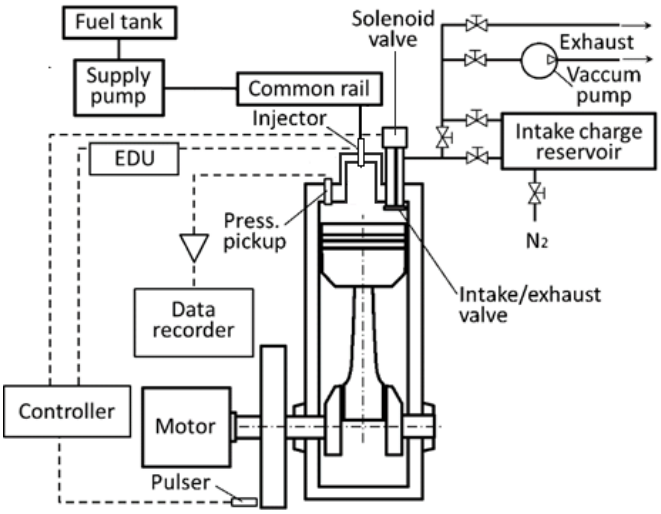

Figure 1. Schematic diagram of experimental setup.

A cuboid combustion chamber (length 30 mm, width 43 mm, height 40 mm) was obtained, as shown in Figure 2. However, the optical field was an area with a length of 30 mm and a height 40 mm. Glass windows were set on three sides of the chamber for visualization experiments. The injector was set perpendicular to the cylinder axis, and details of the operating conditions and injection parameters are shown in Table 1. Among them, the injection parameters of an injection pressure of 80 MPa and injection mass of 0.50 mg by the injector with nozzle diameter 0.12 mm were set as the standard injection conditions. For the fuel injection, a single-hole piezo injector (Denso G3P) with an electronic-controlled common-rail injection system was used. The in-cylinder pressure is monitored by a pressure sensor (Kistler 6052B). The signal was processed through a charge amplifier (Kistler 5011B) and transformed to a digital signal by an analog-to-digital (AD) converter then sent to the computer. Before the experiment, the intake valve was closed, and the reservoir tank and pipe line connecting it with the intake valve were evacuated by a vacuum pump. Then the reservoir tank was filled with nitrogen. The pre-charged gas affects the TDC pressure significantly. For this reason, the tank pressure was measured by an absolute pressure transducer (Kyowa PAB-A-500KP) with high resolution as well as a strain amplifier (Kyowa DMP-713B). The temperature of the gas in the reservoir tank was kept constant with a thermal isolation material and a ribbon heater covering the tank. Then the intake valve was opened, and the motor started to drive the RCEM. Gases contained in reservoir flowed in and out of the combustion chamber through the intake valve, hence the temperature increased as the reciprocating machine rotated. When the valve temperature reached a particular level, the valve was closed, and one compression stroke began. The fuel was then injected at TDC. The injection rates of various injection parameters were measured by the Zeuch method [9]. Thus, injection rate is originally represented by its wave shape with the unit of MPa/ms. According to the pressure-volume equation,

$$\Delta p = \frac{K}{Vc}\Delta Q \quad (1)$$

where,
Δp = pressure rise,
K = bulk modulus of the fuel,
Vc = volume of the chamber,
ΔQ = injection quantity,

the injection mass is calculated by pressure rise inside the container. Then the unit is modified to mg/ms.

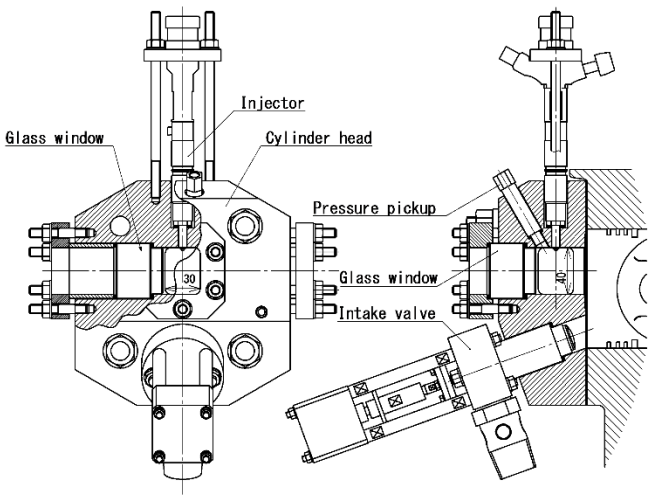

Figure 2. Cross-section of rapid compression and expansion machine.

Two different optical techniques were employed as depicted in Figure 3. The shadowgraph imaging method was employed to the visualization of changes in density of fuel spray. The optical system with a beam of parallel light transmitted through the flow was used for this method. The relatively simple optical setup provided sensitivity to the gradient of index of refraction caused by the difference in density. The Mie scattering method was used to detect the liquid phase of the diesel spray. The light resource was a green (wavelength 532 nm; maximum output 5 W) light-emitting diode. The resolution of images was 555 pixels along injection axle, which corresponded to 40 mm. The images were acquired through a high-speed camera (Photron FASTCAM SA-Z) with a 75 mmØ f1/9.5 lens with no spectral filtering and with the aperture wide open. The camera was triggered at the same timing of the injection signal at TDC. The frame rate was set to 90,000 fps, and the exposure time was 10 μs.

Table 1. Operating conditions and injection parameters.

Injector conditions	
Type	Piezo injector, common-rail
Nozzle	Single-hole
Nozzle hole diameter	0.12, 0.14 mm
Length of nozzle orifice	0.80 mm
Nozzle hole shape	Cylindrical
Injection conditions	
Injection pressure	40, 80, 120 MPa
Injection mass	0.25, 0.50, 0.80 mg
Fuel	JIS#2 Diesel
Ambient conditions at the time of injection	
Ambient pressure	4 MPa
Ambient temperature	850 K
Atmospheric constituent	Nitrogen 100%
Injection timing	TDC

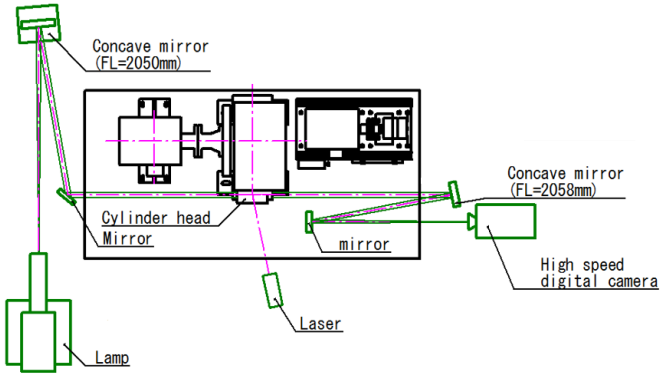

Figure 3. Schematic diagram of optical system.

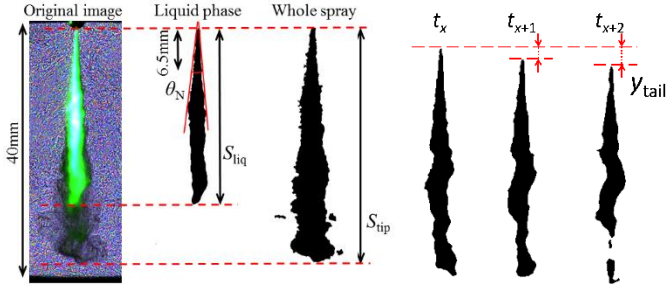

Figure 4. Definition of S_{tip}, S_{liq}, y_{tail}, and θ_N.

The distribution of scattered light on the original images corresponded to the distribution of liquid phase in a spray. As shown in Figure 4, the original images were processed to separate liquid phases. Then the image was also binarized to the whole spray, including both liquid phase and vapor phase. After these processes, spray tip penetration S_{tip}, spray liquid penetration S_{liq}, spray tail position y_{tail}, and near-nozzle spray angle θ_N were measured. θ_N was measured between the tangent lines fitted through the upstream 6.5 mm (90 pixel) of the liquid phase contour. This θ_N can be referred to as the spray angle input for the spray model. y_{tail} refers to the distance from the nozzle tip to the tail of the spray liquid phase after the end of injection, according to Figure 4. Knox et al. indicated that the injection rate shape at the end of injection is a significant factor affecting spray combustion and soot formation following it [10]. Also, previous study suggested that the overlap of pilot spray flame with main spray should be avoided to suppress soot emission. Therefore, the relationship between the development of the lean mixture at spray tail and the injection patterns need to be discussed. Thus, in this study, y_{tail} was defined to compare the spray mixing and vaporizing process at different injection conditions. Also, the spray was modulated as piled disks with height of 1 pixel, as shown in Figure 5. Thus, the volume of spray, V_s, can be calculated as the sum of disks' volume. Then a cone with volume V_s and height S_{tip} was proposed. The cone angle of the composed cone was defined as spray cone angle θ_C, as illustrated in Figure 5. By this approximation method, since the spray volume included the injected fuel as well as the entrained air, the spray entrainment level could be estimated by comparing the θ_C at various injection conditions.

For each injection condition, optical experiments were performed at least ten times, and one fair result close to the average was chosen as the representative.

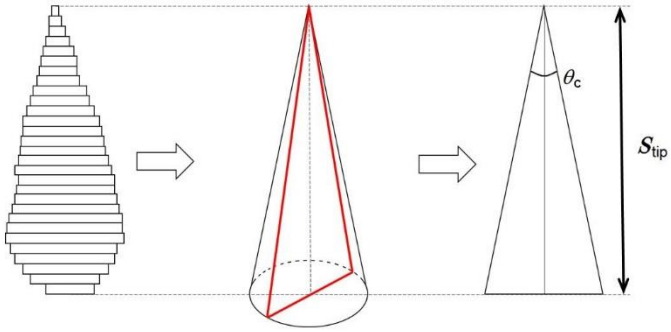

Figure 5. Definition of θ_C.

Experimental Results

Characteristics of Quasi-Steady Injection

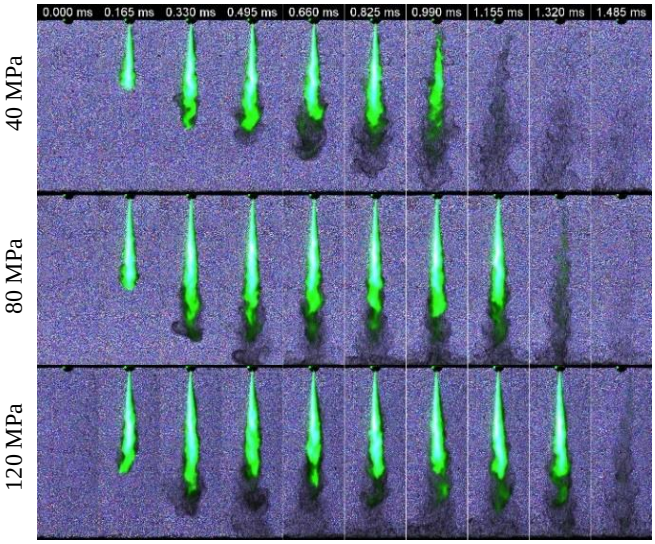

Figure 6. Spray images sequence of quasi-steady injection taken by shadowgraph imaging method and Mie scattering.

Before analyzing the characteristics of small-quantity injection, we investigated the characteristics of injection with rather long injection

duration, which included quasi-steady stage of injection rate as a reference. The injector diameter and injection signal duration were set to 0.12 mm and 400 μs, respectively, while the injection pressure is modified from 40 to 80 to 120 MPa. The original image sequences are shown in Figure 6 and the results of S_{tip}, S_{liq}, and y_{tail} as a function of time ASOI (after start of injection) are shown in Figure 7. The maximum value in the y-axis was set to 35 mm while the whole optical length was 40 mm, as mentioned before. As the spray tip penetrated, the interaction with the chamber wall may affect the characteristics of spray development. Hence, the spray tip penetration was only counted up to 35 mm. Key observations were as follows. Firstly, it could be confirmed that as the injection pressure increased, the spray liquid length reached steady region earlier. Secondly, though S_{liq} fluctuated approximately 2.5 mm during the steady region, no apparent differences were observed among each injection pressure. The result that injection pressure had little effect on average liquid length was consistent with previous experimental results [11] as well as the theoretical analysis based on turbulent spray theory and conservation of momentum [12].

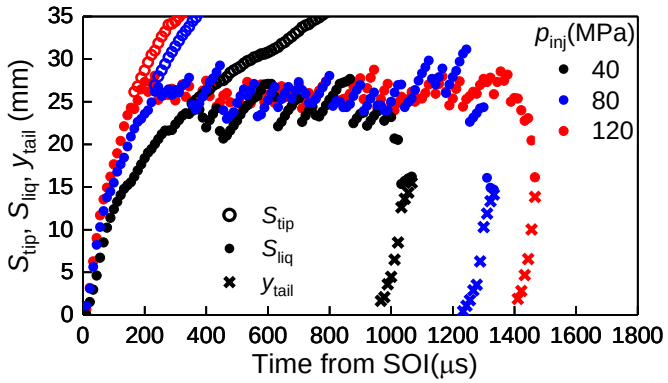

Figure 7. S_{tip}, S_{liq}, and y_{tail} of quasi-steady injection with injection pressure of 40, 80, 120 MPa (ambient temperature 850 K; ambient pressure 4 MPa; injector nozzle diameter 0.12 mm).

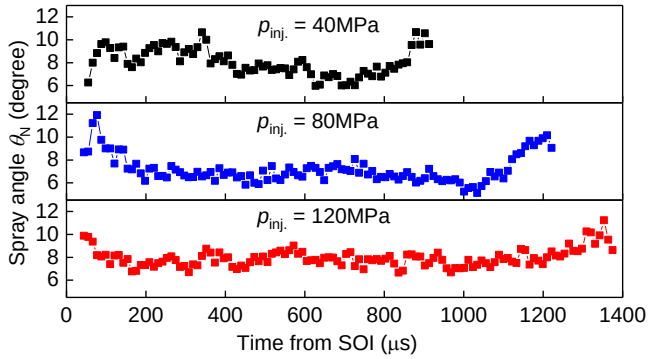

Figure 8. θ_N of quasi-steady injection with injection pressure of 40, 80, 120 MPa (ambient temperature 850 K; ambient pressure 4 MPa; injector nozzle diameter 0.12 mm).

The θ_N are illustrated in Figure 8. Overall, the θ_N starts from 10 to 12° and decreased as injection continued. It then stabilized at approximately 6 to 8°. Only focusing on the end of injection period, it could be noticed that the θ_N increased steadily for all the conditions. The large θ_N value during the initial and terminal stages of injection may have been due to the cavitation effect in the nozzle sac since the needle lift was small during that time [13]. Another hypothesis is that at the beginning of injection, fuel droplets were injected into the quiescent air, which pushed the air in front of the nozzle hole. Therefore, the fuel spray was retarded and pushed in the radial direction [14]. Some differences between each injection pressure were also found. For the injection pressure of 40 MPa, the decrease of θ_N was rather gradual compared to those of higher injection pressure experiments.

Effect of Injection Mass to the Characteristics of Diesel Spray

In this section, the effect of the injection mass on the characteristics of diesel spray was examined with the injection pressure fixed to 80 MPa. The diameter of the injector nozzle hole was 0.12 mm, and injection mass ranged from 0.25 to 0.50 to 0.80 mg. The change in injection mass was achieved by changing the injection signal duration. Thus, the longer injection duration condition corresponded to a larger injection mass condition. The injection rate shape of each injection pattern is shown in Figure 9. The maximum level of injection rate of 0.25 mg injection was lower when compared to other injection conditions. The shape of the injection rate wave of the 0.25 and 0.50 mg injections were similar to a triangle, which is a typical injection rate shape for small-quantity injection. On the other hand, the shape of the 0.80 mg injection had a quasi-steady region where the injection rate stabilized for approximately 100 μs.

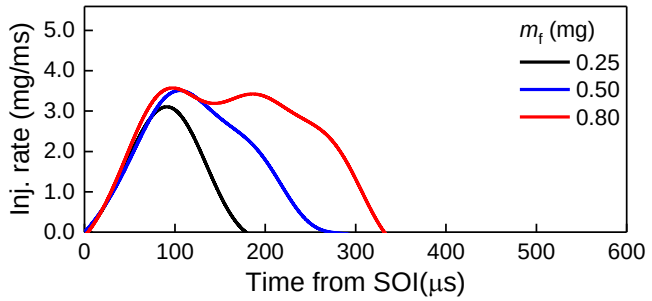

Fig 9. Injection rate shape with various injection mass at injection pressure of 80 MPa (ambient temperature 850 K; ambient pressure 4 MPa; injector nozzle diameter 0.12 mm).

Before comparing the experimental results under different test conditions, the mean and 2σ standard deviation of S_{tip} and S_{liq} and θ_N are shown in Fig 10 and 11, respectively. Only the data of standard injection condition with injection pressure of 80 MPa, injection mass of 0.50 mg, and nozzle diameter of 0.12 mm is shown as an example since the deviations of the acquired data are similar with each other. Among all the experimental results, only one result close to the mean value was chosen to make comparison and discussion.

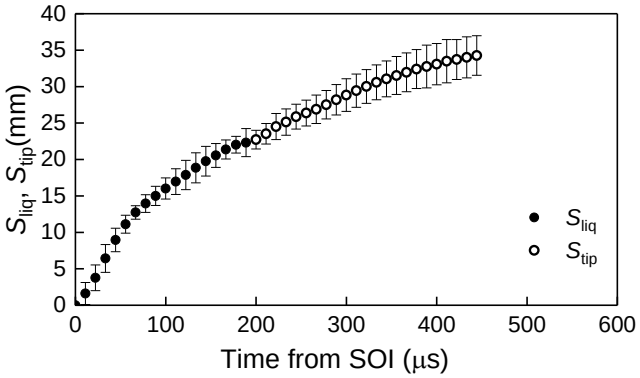

Figure 10. The mean S_{tip} and S_{liq}, of diesel spray with standard injection condition (injection pressure 80 MPa, injection mass 0.50 mg, injector nozzle 0.12 mm). The error bars represent the 2σ standard deviation interval of the mean penetration.

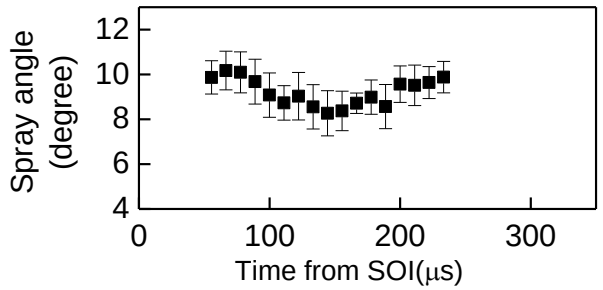

Figure 11. The mean θ_N of diesel spray with standard injection condition (injection pressure 80 MPa, injection mass 0.50 mg, injector nozzle diameter 0.12 mm). The error bars represent the 2σ standard deviation interval of the mean value.

The S_{tip}, S_{liq}, and y_{tail} results under different test conditions are shown in Figure 12. This figure indicates that at the initial stage of the injection, the development of S_{liq} until 200 μs ASOI showed no difference as the changes of injection mass. However, S_{liq} of injection with triangular injection rate shape did not reach the average S_{liq} of quasi-steady injection mentioned in the analysis of Figure 7. Thus, the maximum liquid penetration can be reduced by shortening the injection duration so that the spray impingement problem can be improved. After EOI, S_{liq} decreased and joined with y_{tail}. The speed of S_{tip} development of 0.25 mg injection decreased from about 200 μs ASOI, followed by a 0.50 mg injection at 350 ASOI. y_{tail} of each injection condition as a function of time from EOI is summarized in Fig. 13. As can be seen in the figure, y_{tail} almost developed at the same speed for all the conditions. Hence, it can be concluded that injection mass has no impact on the development of y_{tail}. This conclusion can be explained by the same injection rate decrease shape as shown in Figure 9.

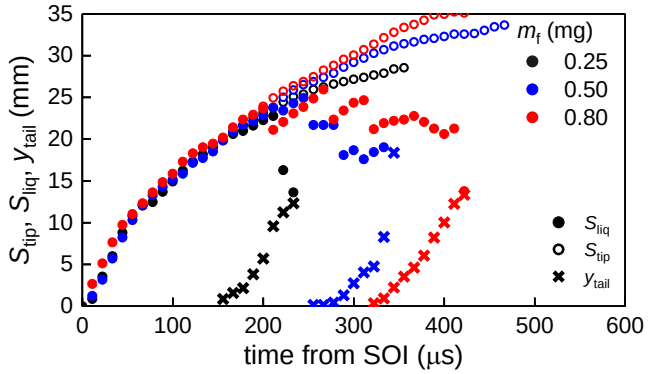

Figure 12. Effect of injection mass on S_{tip}, S_{liq}, and y_{tail}, with injection pressure of 80 MPa (ambient temperature 850 K; ambient pressure 4 MPa; injector nozzle diameter 0.12 mm).

Furthermore, the time dependence characteristics of diesel spray were investigated. Figure 14 shows the log-log chart of S_{tip} and S_{liq} plotted on Figure 10. In order to discern S_{tip} from S_{liq}, the S_{tip} data was plotted in lighter color than S_{liq}. According to the previous experimental results and theoretical analysis, it is commonly believed that the spray tip penetration starts at t dependence and turns to $t^{1/2}$ dependence for a typical quasi-steady injection. Then, at approximately twice of the duration from SOI to injection rate peak, the spray tip penetration function gradually changed to $t^{1/4}$ dependence. In this study, according to Figure 14, the spray tip penetration shows one or steeper dependence on time at the initial stage of injection. The over one dependence on time of spray tip was because the spray tip experienced an accelerating stage as J. Kostas et al. suggested [6]. Then, at a later stage, a square-root dependence on time was observed. It should be noted that some time after EOI, the spray tip penetration developed as a function of $t^{1/4}$ when injection mass was 0.25 mg and 0.50 mg. This trend of spray tip penetration was more obvious if we focused on the latter part of the injection by changing the time scale, as shown in Figure 14. For the case of injection mass of 0.80 mg, it was supposed that the $t^{1/4}$ dependence of spray tip penetration was not observed because the spray tip reached the limitation of optical access before the change in time dependence could be recognized. The timing when the dependence on time gradually changed from 1 to 1/2 was approximately 70 μs to 80 μs for all the injection condition.

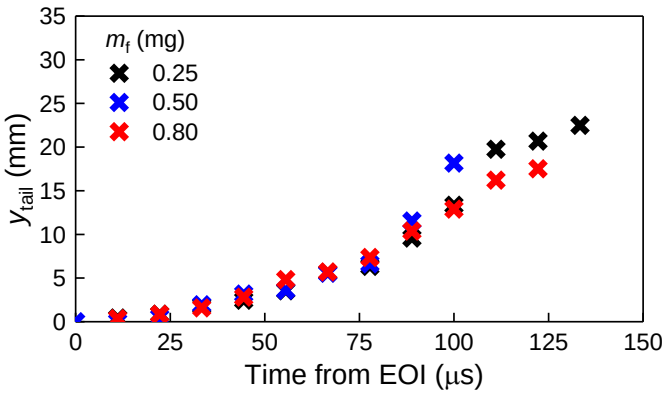

Figure 13. y_{tail} with various injection mass a t injection pressure of 80 MPa (ambient temperature 850 K; ambient pressure 4 MPa; injector nozzle diameter 0.12 mm).

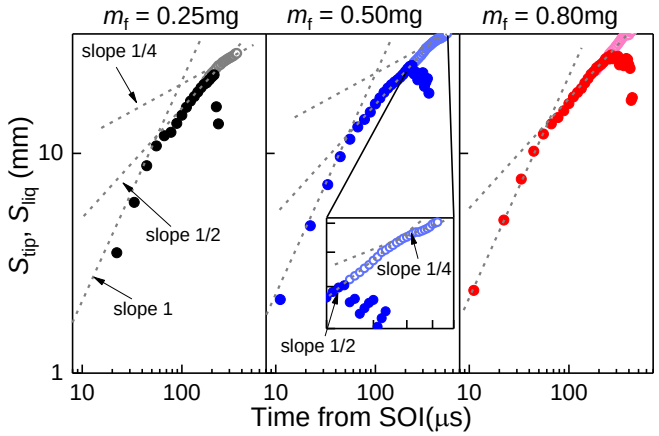

Figure 14. Log-log chart of S_{tip}, S_{liq} with various injection mass at injection pressure of 80 MPa (ambient temperature 850 K; ambient pressure 4 MPa; injector nozzle diameter 0.12 mm).

The θ_N is illustrated in Figure 15. A similar trend to quasi-steady injection is observed for the injection masses of 0.50 mg and 0.80 mg. Namely, the θ_N decreased from a rather large value and then increased toward the end of injection. However, in the case of the smallest injection mass, the increase of θ_N was not observed. The θ_N starts from over 10°, and then decreases slightly during the entire injection process. According the previous study about spray angle using a multi-hole injector, the following hypothesis can be made [13]. The flow in a sac during the entire injection duration is unstable when the injection mass is too small. However, in order to explain this phenomenon clearly in detailed description, further study is needed.

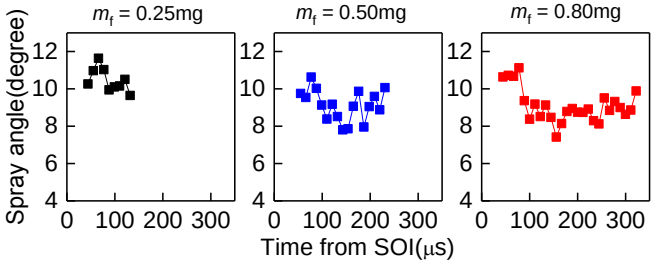

Figure 15. Effect of injection mass on θ_N (ambient temperature 850 K; ambient pressure 4 MPa; injector nozzle diameter 0.12 mm).

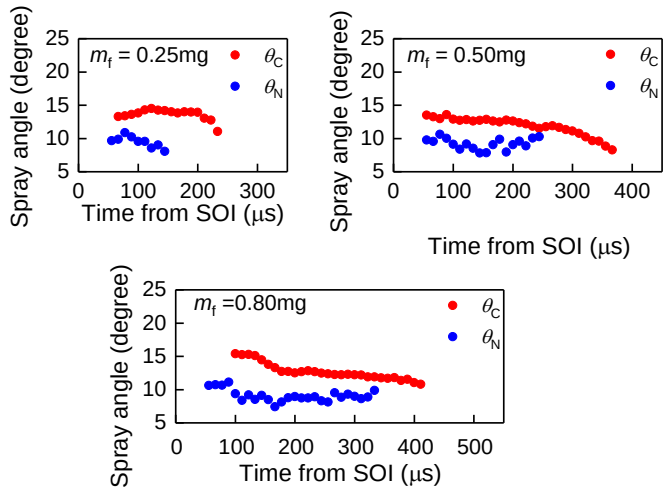

Figure 16. The comparison of θ_N and θ_C with various injection mass at injection pressure of 80 MPa (ambient temperature 850 K; ambient pressure 4 MPa; injector nozzle diameter 0.12 mm).

The θ_N and θ_C are compared in Figure 16. Overall, θ_C was 5° larger than θ_N. For all of the experimental conditions, θ_C maintained constant value or decreased gradually from SOI. A noticeable decrease in θ_C is observed after EOI. At the initial stage of the injection, since the vaporization of the spray was insufficient, θ_C was mainly influenced by the development of spray liquid phase. Therefore, in order to investigate the effect of spray vaporization and mixing process on spray dispersion for each injection conditions, we should focus on the period when the spray vapor phase was fully developed and separated from the liquid phase. According to the history of S_{tip} and S_{liq} (Figure 10), this period started from about 180 μs ASOI. The observation of θ_C from 180 μs ASOI showed that, except for the 0.25 mg injection for which injection had already ended before 180 μs ASOI, there were little differences concerning the value of θ_C.

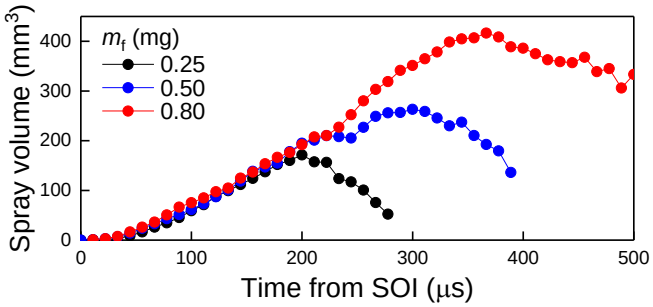

Figure 17. Spray volume with various injection mass (ambient temperature 850 K; ambient pressure 4 MPa; injector nozzle diameter 0.12 mm).

Spray volume as function of time ASOI is illustrated in Figure 17. At the initial stage from SOI to 200 μs ASOI, the history of spray volume increase for different injection conditions was exactly the same. Also, the spray volume decreased after end of injection. This decrease actually did not indicate that the spray volume itself was decreasing. In fact, due to the over-lean of the fuel spray and the decrease of fuel-air mixing speed after EOI, the "spray area" detected by shadow graph imaging method decreased.

Effect of Injection Pressure to the Characteristics of Diesel Spray

In this section, the effect of the injection pressure on the characteristics of the diesel spray is examined with the injection mass fixed to 0.50 mg. The diameter of the injector nozzle hole was 0.12 mm and the injection pressure was varied from 40 to 80 to 120 MPa. The injection rate wave shape of each injection pattern is illustrated in Figure 18. The injection duration decreased as the injection pressure increased. On the other hand, the maximum level of the injection rate increased with injection pressure. The 120 MPa injection had the sharpest increase and decrease in injection rate shape according to Figure 18. The 40 MPa injection condition had a relatively steady region in injection rate while the others did not.

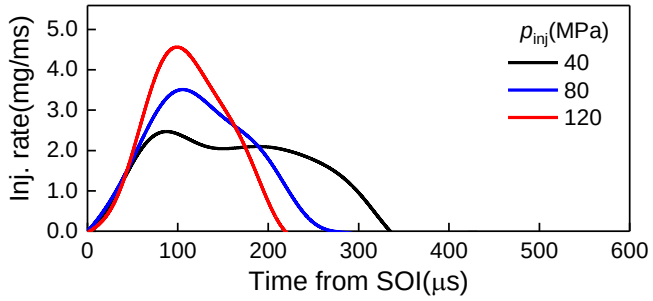

Figure 18. Injection rate shape with various injection pressure at injection mass of 0.50 mg (ambient temperature 850 K; ambient pressure 4 MPa; injector nozzle diameter 0.12 mm).

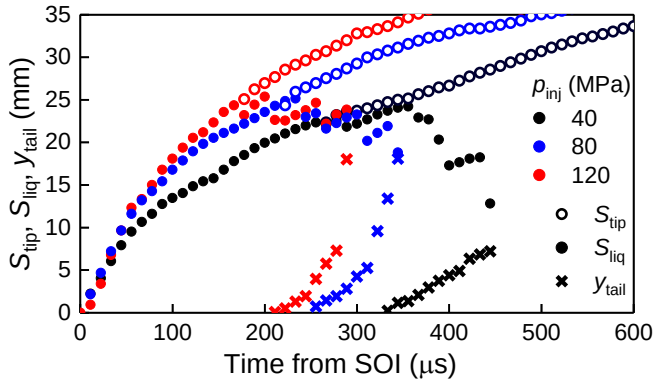

Figure 19. Effect of injection pressure on S_{tip}, S_{liq}, and y_{tail}, with injection mass of 0.50 mg (ambient temperature 850 K; ambient pressure 4 MPa; injector nozzle diameter 0.12 mm).

The S_{tip}, S_{liq}, and y_{tail} results under different test conditions are shown in Figure 19. Though S_{liq} development showed differences from the start of injection, the maximum S_{liq} showed no difference during the change of injection pressure. From 0 to 50 μs ASOI, the injection rate was close among various injection pressures, hence S_{liq} development was also similar. At 50 μs ASOI, S_{liq} development of the 0.25 mg injection started to decrease and deviated from the other injection

conditions as the injection rate difference began to increase. Then the S_{liq} development of the 0.50 mg injection separated from that of the 0.80 mg injection at about 120 μs ASOI. Hence, as the increasing of injection rate stopped, the spray tip penetration development showed a decrease.

The y_{tail} of each injection condition was studied to clarify the effect of differences on the injection pressure of fuel-air mixing from the injector nozzle after EOI. The y_{tail} of each injection condition as a function of time from EOI is summarized in Figure 21. Higher injection pressure led to the faster y_{tail} development. This trend can be explained as follows. The spray velocity near the nozzle was higher for injection with higher pressure. Therefore, the liquid phase fuel moved faster after EOI with higher injection pressure. Also, the high injection pressure had a sharp ramp-down of injection rate. Consequently, the air entrainment by the end of injection was stimulated. Hence, compared to the lower injection conditions, fuel rarefication and vaporization were faster near the injector nozzle [10].

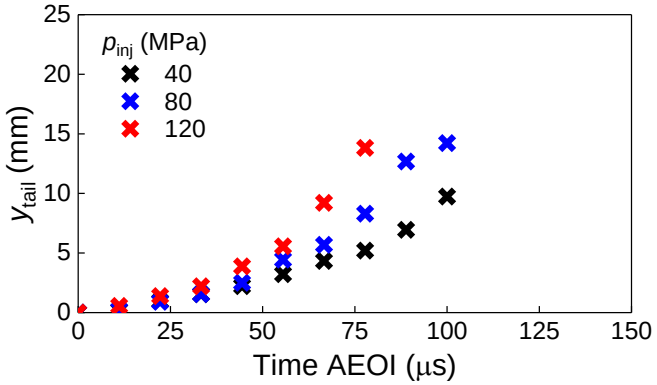

Figure 21. y_{tail} with various injection pressure at injection mass of 0.50 mg (ambient temperature 850 K; ambient pressure 4 MPa; injector nozzle diameter 0.12 mm).

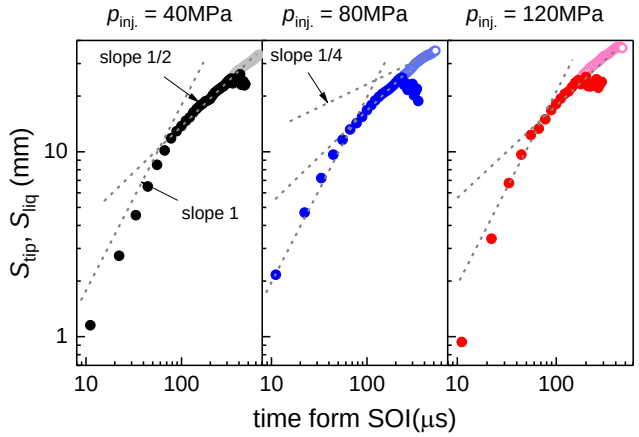

Figure 21. Log-log chart of S_{tip}, S_{liq} with various injection pressure at injection mass of 0.50 mg (ambient temperature 850 K; ambient pressure 4 MPa; injector nozzle diameter 0.12 mm).

The time dependence characteristics of diesel spray are examined in Figure 21 by comparing the log-log chart of S_{tip} and S_{liq} plot under different injection pressures. During the initial stage of injection, the spray tip penetration started from t dependence and then changed to $t^{1/2}$. 120 MPa injection showed slightly earlier dependence change compared to the 40 MPa and 80 MPa injections. The dependence of spray tip penetration as a function of $t^{1/4}$ was only observed in 80 MPa. It is considered that for the higher injection pressure condition, the spray tip penetrated faster so that the spray tip reached the limitation of visualization before the change in time dependence. For the lower injection pressure condition, the spray tip had grown too lean to be recognized before the $t^{1/4}$ dependence could be identified.

The θ_N is illustrated in Figure 22. The θ_N started from approximately 10 to 11° at the beginning of the injection. Then θ_N decreased to 8° for the injection with pressures of 80 MPa and 120 MPa. However, this decrease could not be clearly confirmed in the lowest injection pressure condition. At this injection pressure, the θ_N ranged from 9 to 10° through the entire injection duration.

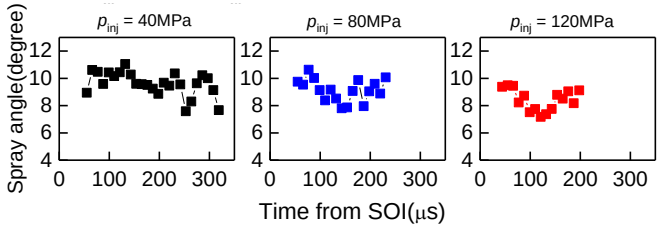

Figure 22. The effect of injection pressure on θ_N (ambient temperature 850 K; ambient pressure 4 MPa; injector nozzle diameter 0.12 mm).

The θ_N and θ_C are compared in Figure 23. The overall trend of θ_C was similar among each injection pressure as θ_C decreased through the injection. As the same reason referred in the analysis of Figure 16, we focused on the period when spray vapor phase was fully developed and separated from the liquid phase. The finding was that θ_C decreased following the increase of injection pressure.

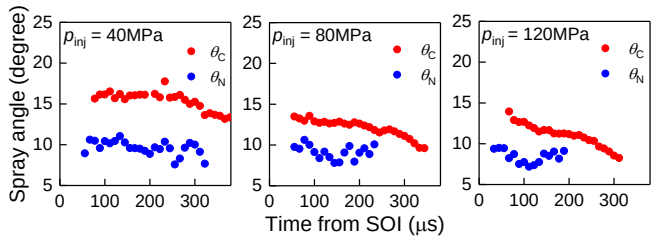

Figure 23. The comparison of θ_N and θ_C with various injection pressure at injection mass of 0.50 mg (ambient temperature 850 K; ambient pressure 4 MPa; injector nozzle diameter 0.12 mm).

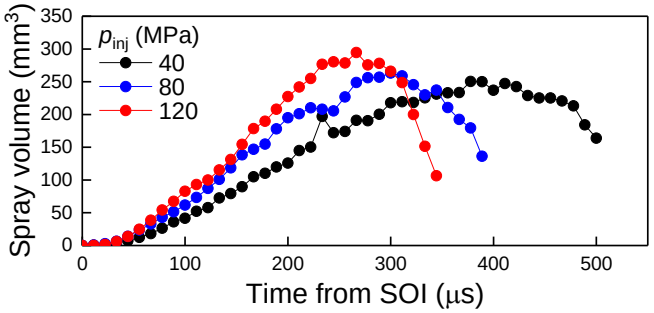

Figure 24. Spray volume with various injection pressure (ambient temperature 850 K; ambient pressure 4 MPa; injection mass 0.50 mg).

Spray volume as a function of time ASOI is illustrated in Figure 24. The spray volume continued to increase even after EOI. The spray volume increase rate and maximum spray volume grew higher as the injection pressure increased from 40 MPa to 120 MPa. When looking at about 250 μs ASOI, according to injection rate shape in Figure 18, the injected mass was almost the same for all of the injection

conditions. At this time, the spray volume was larger for higher injection conditions. Therefore, it can be inferred that air entrainment could be enhanced by increasing injection pressure.

Effect of Injector Nozzle Hole Diameter to the Characteristics of Diesel Spray

In order to clarify the effect of injector nozzle hole diameter to spray characteristics, injection pressure and mass condition were fixed to 80 MPa and 0.50 mg, respectively, while two injectors with nozzle hole diameters of 0.12 mm and 0.14 mm were utilized in this section. The injection rate shapes are illustrated in Figure 25, and experimental results of the spray tip penetrations are presented in Figure 26. According to Figure 25, the injection duration was shorter, and the maximum injection rate level was higher in larger nozzle hole diameter conditions.

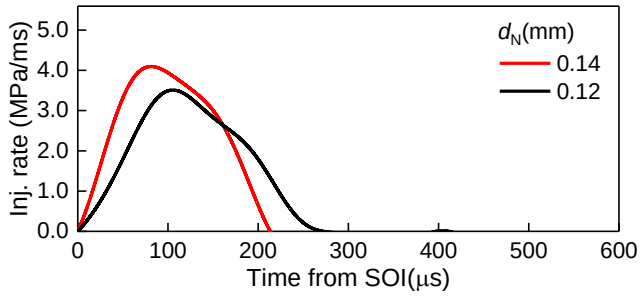

Figure 25. Injection rate shape with nozzle hole diameter 0.12 mm and 0.14 mm at injection mass 0.50 mg and injection pressure 80 MPa (ambient temperature 850 K; ambient pressure 4 MPa).

At the initial stage of injection, S_{liq} for different two injector nozzle hole diameters showed little difference until about 80μs after SOI in Figure 26. The spray tip penetration then deviated, and 0.14 mm injection developed faster. At the initial stage, theoretically, the spray tip penetration is only dependent on injection pressure. Since the injection pressure was the same, the experimental results of spray tip penetration showed the same increase trend as expected. After the spray tip was fully atomized and vaporized, the momentum conservation equation could be adopted and spray tip penetration developed as a function of $t^{1/2}$. During this period the tip penetration was dependent on 1/2 power of the nozzle hole diameter [15]. In addition, when comparing the average S_{liq} during its steady region, it could be noticed that larger nozzle diameter led to longer S_{liq}. This trend corresponded well with the previous research conducted by Peyri, R. [12].

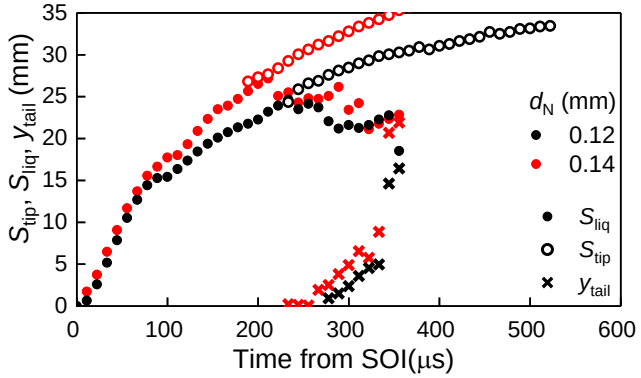

Figure 26. Effect of nozzle diameter on S_{tip}, S_{liq}, and y_{tail} with injection mass of 0.50 mg and injection pressure 80 MPa (ambient temperature 850 K; ambient pressure 4 MPa).

θ_N is compared in Figure 27. For both injection conditions, the θ_N decreased from SOI, reaching a minimum value around 150 μs ASOI, and increased towards EOI. However, the initial near-nozzle spray angle was 3° larger for injection with a nozzle hole diameter of 0.14 mm. In addition, θ_C and θ_N were compared to investigate the effect of the injector nozzle hole diameter on spray characteristics in Figure 27. At the initial stage of injection, the θ_C of 0.14 mm nozzle hole diameter injection was larger since θ_N was larger, as mentioned before. However, after the spray vapor phase is fully developed, approximately 200μs ASOI according to Figure 26, no influence of nozzle hole diameter on θ_C was validated.

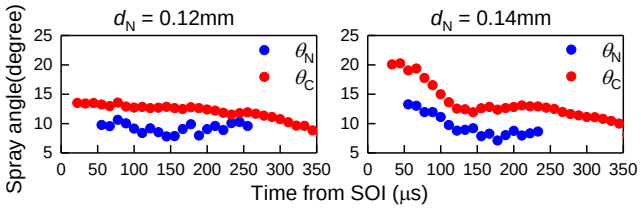

Figure 27. The comparison of θ_N and θ_C with different nozzle hole diameters (ambient temperature 850 K; ambient pressure 4 MPa; injection pressure 80MPa; injection mass 0.50mg).

Summary

In this study, a rapid compression and expansion machine was used to investigate the characteristics of diesel spray. The injection pressure (40, 80, 120 MPa), injection mass (0.25, 0.50, 0.80 mg), and injector nozzle diameter (0.12, 0.14 mm) were modified for the optical experiments. The shadowgraph imaging method and Mie scattering method were used to visualize the development of spray liquid and vapor phase simultaneously. The spray vapor tip penetration (S_{tip}), spray liquid penetration (S_{liq}), spray tail position (y_{tail}), near-nozzle spray angle (θ_N), and spray cone angle (θ_C) were analyzed from the spray images taken from a high-speed camera and compared with that of quasi-steady injections. The summaries of spray characteristics of small-quantity injection are listed as following:

1. For the case of the same injection rate rise, when injection mass is changed by modifying injection duration with constant nozzle hole diameter and injection pressure, the injection mass had no effect on the spray tip penetration development during the initial stage of injection. Except for the injection mass of 0.80 mg, the spray liquid phase did not reach the average liquid length of quasi-steady injection for small-quantity injection conditions.
2. The spray tip penetration showed one or more than one dependence on time at the initial stage of injection, then soon followed a functional fit of t. After that, the spray tip penetration was found to be proportional to $t^{1/2}$. Furthermore, it should be noted that some time after EOI, spray tip penetration developed as a function of $t^{1/4}$.
3. When injection pressure was the same, the injection rate decrease rate was the same during the terminal stage of injection. Hence, the spray tail position development followed the same history. However, when the injection pressure increased, the entrainment near the nozzle was accelerated at the end of the injection. Therefore, compared to lower injection pressure conditions, the spray tail position developed faster.
4. The near-nozzle spray angle starts at over 10° and decreased from the start of injection. Then, the near-nozzle spray angle increased towards the end of injection. In addition, a larger injector nozzle diameter could lead to a larger near-nozzle spray angle at the initial stage of injection.

5. The spray cone angle decreased from start of injection and no influence of injection mass and injector nozzle diameter was observed from this study. However, higher injection pressure led to a smaller spray cone angle after the spray vapor phase was fully developed.

References

1. Zhang, L., "A Study of Pilot Injection in a DI Diesel Engine," SAE Technical Paper 1999-01-3493, 1999, doi:10.4271/1999-01-3493.
2. Ogawa, H., et al. "Improvements in Diesel Combustion with After-Injection," *Transactions of Society of Automotive Engineers of Japan* 39.1 (2008): 101-106.
3. Badami, Marco, Federico Millo, and D. D. D'amato. "Experimental investigation on soot and NOx formation in a DI common rail diesel engine with pilot injection," SAE Technical Paper 2001-01-0657, 2001, doi:10.4271/2001-01-0657.
4. Hiroyasu, H. and Arai, M., "Structures of Fuel Sprays in Diesel Engines," SAE Technical Paper 900475, 1990, doi:10.4271/900475.
5. Naber, J. and Siebers, D., "Effects of Gas Density and Vaporization on Penetration and Dispersion of Diesel Sprays," SAE Technical Paper 960034, 1996, doi:10.4271/960034.
6. Kostas, J., D. Honnery, and J. Soria. "Time resolved measurements of the initial stages of fuel spray penetration." *Fuel* 88.11 (2009): 2225-2237. doi:10.1016/j.fuel.2009.05.013.
7. Musculus, M. and Kattke, K., "Entrainment Waves in Diesel Jets," *SAE Int. J. Engines* 2(1):1170-1193, 2009, doi:10.4271/2009-01-1355.
8. Pickett, L., Manin, J., Payri, R., Bardi, M. et al., "Transient Rate of Injection Effects on Spray Development," SAE Technical Paper 2013-24-0001, 2013, doi:10.4271/2013-24-0001.
9. W. Zeuch, Neue Verfahren zur Messung des Einspritzgesetzes und der Einspritz-Regelmaessigkeit von Diesel-Einspritzpumpen, MTZ Johrg. 22 helf 9.1961 [in German].
10. Knox, B. and Genzale, C., "Effects of End-of-Injection Transients on Combustion Recession in Diesel Sprays," *SAE Int. J. Engines* 9(2):932-949, 2016, doi:10.4271/2016-01-0745.
11. Johnson, J., Naber, J., Lee, S., Kurtz, E. et al., "Investigation of Diesel Liquid Spray Penetration Fluctuations under Vaporizing Conditions," SAE Technical Paper 2012-01-0455, 2012, doi:10.4271/2012-01-0455.
12. Payri, R., et al. "Diesel nozzle geometry influence on spray liquid-phase fuel penetration in evaporative conditions." *Fuel* 87.7 (2008): 1165-1176. doi:10.1016/j.fuel.2007.05.058.
13. Gavaises, M. and Andriotis, A., "Cavitation Inside Multi-hole Injectors for Large Diesel Engines and Its Effect on the Near-nozzle Spray Structure," SAE Technical Paper 2006-01-1114, 2006, doi:10.4271/2006-01-1114.
14. Taşkiran, Özgür Oğuz, and Metin Ergeneman. "Experimental study on diesel spray characteristics and autoignition process." *Journal of Combustion* vol. 2011, Article ID 528126, 20 pages, 2011, doi:10.1155/2011/528126.
15. Wakuri, Y., Fujii, M., Amitani, T., Tsuneya, R., "Studies on the Penetration of Fuel Spray of Diesel Engines" *Transactions of the Japan Society of Mechanical Engineers* Vol. 25 (1959) No. 156 P820-826, doi:10.1299/kikai1938.25.820

Contact Information

Zhichao Bao: bao.chishao.64z@st.kyoto-u.ac.jp

Naoto Horibe: horibe@energy.kyoto-u.ac.jp

Takuji Ishiyama: ishiyama@energy.kyoto-u.ac.jp

Acknowledgments

The authors would like to thank Mr. Akifumi Nomura from Kyoto University for his support in setting-up the visualization system and processing images.

Definitions/Abbreviations

ASOI	after start of injection
AEOI	after end of injection
SOI	start of injection
EOI	end of injection
TDC	top dead center
RCEM	rapid compression and expansion machine
p_{atm}	atmospheric pressure
T_{atm}	atmospheric temperature
p_{inj}	injection pressure
m_f	Injection mass
d_N	injector nozzle hole diameter
S_{tip}	spray tip penetration
S_{liq}	spray liquid phase penetration
y_{tail}	distance from nozzle tip to spray tail
θ_N	near-nozzle spray angle
θ_C	spray cone angle
V_s	spray volume